Limit on light gauge boson production in $e^+e^- \to \mu^+\mu^-\gamma$ interactions with the KLOE experiment*

The KLOE-2 Collaboration

D. Babusci [h], I. Balwierz-Pytko [g], G. Bencivenni [h], C. Bloise [h], F. Bossi [h], P. Branchini [r], A. Budano [q,r], L. Caldeira Balkeståhl [u], F. Ceradini [q,r], P. Ciambrone [h], F. Curciarello [i,d], E. Czerwiński [g], E. Danè [h], V. De Leo [i,d], E. De Lucia [h], G. De Robertis [b], A. De Santis [h], P. De Simone [h], A. Di Cicco [q,r], A. Di Domenico [m,n], R. Di Salvo [p], D. Domenici [h], O. Erriquez [a,b], G. Fanizzi [a,b], A. Fantini [o,p], G. Felici [h], S. Fiore [s,n], P. Franzini [m,n], A. Gajos [g], P. Gauzzi [m,n], G. Giardina [i,d], S. Giovannella [h], E. Graziani [r], F. Happacher [h], L. Heijkenskjöld [u] B. Höistad [u], T. Johansson [u], K. Kacprzak [g], D. Kamińska [g], W. Krzemien [g], A. Kupsc [u], J. Lee-Franzini [h,t], F. Loddo [b], S. Loffredo [q,r], G. Mandaglio [i,d,c], M. Martemianov [j], M. Martini [h,ℓ], M. Mascolo [o,p], R. Messi [o,p], S. Miscetti [h], G. Morello [h], D. Moricciani [p], P. Moskal [g], F. Nguyen [r,w], A. Palladino [h], A. Passeri [r], V. Patera [k,h], I. Prado Longhi [q,r], A. Ranieri [b], P. Santangelo [h], I. Sarra [h], M. Schioppa [e,f], B. Sciascia [h], M. Silarski [g], L. Tortora [r], G. Venanzoni [h], W. Wiślicki [v], M. Wolke [u], J. Zdebik [g]

[a] *Dipartimento di Fisica dell'Università di Bari, Bari, Italy.*

[b] *INFN Sezione di Bari, Bari, Italy.*

[c] *Centro Siciliano di Fisica Nucleare e Struttura della Materia, Catania, Italy.*

[d] *INFN Sezione di Catania, Catania, Italy.*

[e] *Dipartimento di Fisica dell'Università della Calabria, Cosenza, Italy.*

[f] *INFN Gruppo collegato di Cosenza, Cosenza, Italy.*

[g] *Institute of Physics, Jagiellonian University, Cracow, Poland.*

[h] *Laboratori Nazionali di Frascati dell'INFN, Frascati, Italy.*

[i] *Dipartimento di Fisica e Scienze della Terra dell'Università di Messina, Messina, Italy.*

Preprint submitted to Physics Letters B *1 May 2014*

[j] *Institute for Theoretical and Experimental Physics (ITEP), Moscow, Russia.*

[k] *Dipartimento di Scienze di Base ed Applicate per l'Ingegneria dell'Università "Sapienza", Roma, Italy.*

[ℓ] *Dipartimento di Scienze e Tecnologie applicate, Università "Guglielmo Marconi", Roma, Italy.*

[m] *Dipartimento di Fisica dell'Università "Sapienza", Roma, Italy.*

[n] *INFN Sezione di Roma, Roma, Italy.*

[o] *Dipartimento di Fisica dell'Università "Tor Vergata", Roma, Italy.*

[p] *INFN Sezione di Roma Tor Vergata, Roma, Italy.*

[q] *Dipartimento di Matematica e Fisica dell'Università "Roma Tre", Roma, Italy.*

[r] *INFN Sezione di Roma Tre, Roma, Italy.*

[s] *ENEA UTTMAT-IRR, Casaccia R.C., Roma, Italy*

[t] *Physics Department, State University of New York at Stony Brook, USA.*

[u] *Department of Physics and Astronomy, Uppsala University, Uppsala, Sweden.*

[v] *National Centre for Nuclear Research, Warsaw, Poland.*

[w] *Present Address: Laboratório de Instrumentação e Física Experimental de Partículas, Lisbon, Portugal.*

Abstract

We have searched for a light vector boson U, the possible carrier of a "dark force", with the KLOE detector at the DAΦNE e^+e^- collider, motivated by the astrophysical evidence for the presence of "dark matter" in the universe. Using e^+e^- collisions collected for an integrated luminosity of 239.3 pb^{-1}, we look for a dimuon mass peak in the reaction $e^+e^-\to\mu^+\mu^-\gamma$, corresponding to the decay $U\to\mu^+\mu^-$. We find no evidence for a U vector boson signal. We set a 90% CL upper limit for the kinetic mixing parameter ϵ^2 of 1.6×10^{-5} to 8.5×10^{-7} for the mass region $520 < m_U < 980$ MeV.

Key words: dark matter, dark forces, U boson, upper limit

⋆ This paper is dedicated to the memory of Juliet Lee-Franzini.

Email addresses: fcurciarello@unime.it (F. Curciarello), gmandaglio@unime.it (G. Mandaglio), graziano.venanzoni@lnf.infn.it (G. Venanzoni).

1 Introduction

Astronomical observations establish beyond any reasonable doubt the presence in the universe of mass in large excess over the amount required by the observed light or other em radiation emission or absorption, by more than a factor of five [1]. Dark matter is at present detected only by its gravitational effects on large astronomical bodies and its nature remains as yet unknown. It is also well established that baryons can only contribute minutely to dark matter. If the dark matter consists of some new kind of particles which carry some new kind of charge we might expect its current to couple to some new kind of vector boson gauge field. Explicit models have been constructed in which the vector boson might be as light as few MeV to few GeV. The dark force vector boson might weekly couple [1–4] to the Standard Model sector whose particle might carry tiny amount of the new charge above. The possible existence of a new gauge vector boson U, of $\mathcal{O}(1)$ GeV mass, associated with dark matter particles, could explain [5–7] several puzzling effects observed by astrophysics experiments [8–14]. The U boson couples with the ordinary photon [15] through kinetic mixing, with a mixing parameter ϵ which measures the *dark charge* of SM particles normalized to their electric charge [1].

High luminosity e^+e^- colliders are ideal tools for the search of the U Boson [16–18] because they provide a clean environment, high-statistics and good understanding of background. A particularly clean channel is the reaction $e^+e^- \to U\gamma$ followed by the decay $U \to \ell^+\ell^-$, where $\ell = e,\ \mu$ [19]. Production of U Boson would result in a peak in the dilepton invariant mass spectrum. The $U\gamma$ production process allows one to reach a sensitivity for the mixing parameter ϵ in the range $\{10^{-3}\text{-}10^{-2}\}$, for U-boson masses, m_U, up to a few GeV [2–4, 19].

The search for a U-boson signal described in the following employs data collected in 2002 with the KLOE detector at DAΦNE, running at the ϕ-meson peak, for an integrated luminosity of 239.3 pb^{-1}. We limit our search to the muon channel, searching for a peak in the dimuon mass spectrum. The process $e^+e^-\to\mu^+\mu^-\gamma$ receives a very large contribution from the reaction $e^+e^-\to\mu^+\mu^-$ with additional photon emission by electrons or muons, usually called initial and final state radiation or ISR and FSR. Kinematical and geometrical cuts strongly suppress the FSR contribution. The ISR contribution can be written as

$$\frac{\mathrm{d}\sigma_{\mu\mu\gamma}}{\mathrm{d}\sqrt{s_\mu}} = \sigma(e^+e^- \to \mu^+\mu^-, \sqrt{s_\mu}) \times H\,, \tag{1}$$

[1] This goes back to 1932, Jan Oort, and 1933, Fritz Zwicky.

where $\mathrm{d}\sigma_{\mu\mu\gamma}/\mathrm{d}\sqrt{s_\mu}$ is the differential cross section for $e^+e^- \to \mu^+\mu^-\gamma$ as a function of the dimuon invariant mass $\sqrt{s_\mu}$ or $M_{\mu\mu}$, and H is the radiator function. H has been obtained from QED including NLO corrections [20–24]. Comparison with the measured cross section allows the extraction of a limit for ϵ.

2 The KLOE Detector

The KLOE detector operates at DAΦNE, the Frascati ϕ-factory. DAΦNE is an e^+e^- collider usually operated at a center of mass energy, $W \sim m_\phi \sim 1.019$ GeV. Positron and electron beams collide at an angle of $\pi - 25$ mrad, producing ϕ mesons nearly at rest. The KLOE detector consists of a large cylindrical drift chamber (DC) [25], surrounded by a lead-scintillating-fiber electromagnetic calorimeter (EMC) [26]. A superconducting solenoid surrounding the EMC provides a 0.52 T magnetic field along the axis of the drift chamber which coincides with the bisector of the electron and positron beams which we also take as the z-axis.

The EMC barrel and end-caps cover 98% of the solid angle. Calorimeter modules are read out at both ends by 4880 photomultipliers. Energy and time resolutions are $\sigma_E/E = 0.057/\sqrt{E(\mathrm{GeV})}$ and $\sigma_t = 57$ ps$/\sqrt{\mathrm{E(GeV)}} \oplus 100$ ps, respectively. The drift chamber has only stereo sense wires and is 4 m in diameter, 3.3 m long. It is built out of carbon-fibers and operates with a low-Z gas mixture (helium with 10% isobutane). Spatial resolutions are $\sigma_{xy} \sim 150$ μm and $\sigma_z \sim 2$ mm. The momentum resolution for large angle tracks is $\sigma(p_\perp)/p_\perp \sim 0.4\%$. The trigger uses both EMC and DC information. Events used in this analysis are triggered by at least two energy deposits larger than 50 MeV in two sectors of the barrel calorimeter [27].

3 Event Selection

A $\mu\mu\gamma$ candidate must have two tracks of opposite sign curvature, crossing a cylinder of radius 8 cm and length 15 cm centered at the interaction point, with $50^\circ < \theta < 130^\circ$ and an undetected photon whose momentum, computed from the two track values according to the $\mu\mu\gamma$ kinematics, points at small polar angle ($\theta < 15^\circ$, $> 165^\circ$) [28]. These requirements limit the range of $M_{\mu\mu}$ to be larger than 500 MeV. This separation between the tracks and photon-emission regions greatly reduces the contamination from the resonant process $e^+e^- \to \phi \to \pi^+\pi^-\pi^0$, where charged pions are misidentified as muons and the π^0 mimics the missing momentum of the photon(s), and from the

FSR processes $e^+e^- \to \pi^+\pi^-\gamma_{\rm FSR}$ and $e^+e^- \to \mu^+\mu^-\gamma_{\rm FSR}$. ISR photons are strongly peaked along the beam line. The above requirements are also satisfied by $e^+e^- \to e^+e^-\gamma$ radiative Bhabha events. A particle identity estimator (L_i), based on a pseudo-likelihood function using time-of-flight and calorimeter information (size and shape of the energy deposit) is used to obtain additional separation between electrons and pions or muons [29, 30].

Events with both tracks satisfying $L_i < 0$ are rejected as $e^+e^-\gamma$. The signal loss due to this requirement is less than 0.05%, as evaluated using $\mu^+\mu^-$ samples obtained from both measured data and from Monte Carlo (MC) simulation. Pions and muons are identified by means of the variable $M_{\rm trk}$, the mass of particles x^+, x^- in the $e^+e^- \to x^+x^-\gamma$ process where we assume the presence of an unobserved photon and that the tracks belong to particles of the same mass and momentum equal to the observed value. The $M_{\rm trk}$ ranges 80–115 and >130 MeV identify muons and pion.

At the end of the analysis chain for the $\mu^+\mu^-\gamma$ selection, residual backgrounds consisting of $e^+e^-\to e^+e^-\gamma$, $e^+e^-\to\pi^+\pi^-\gamma$ and $e^+e^-\to\phi\to\pi^+\pi^-\pi^0$ are still present. The residual background is obtained by fitting the observed $M_{\rm trk}$ spectrum with a superposition of MC simulated distributions describing signal plus $\pi^+\pi^-\gamma$, $\pi^+\pi^-\pi^0$ backgrounds, and a distribution obtained from data for the $e^+e^-\gamma$ [28]. Additional background from $e^+e^-\to e^+e^-\mu^+\mu^-$ and $e^+e^-\to e^+e^-\pi^+\pi^-$ has been evaluated. The $e^+e^-\to e^+e^-\pi^+\pi^-$ contribution is negligible while $e^+e^-\to e^+e^-\mu^+\mu^-$ is at the percent level below 0.54 GeV and decreases with $M_{\mu\mu}$. Figure 1 shows the fractions of the background processes,

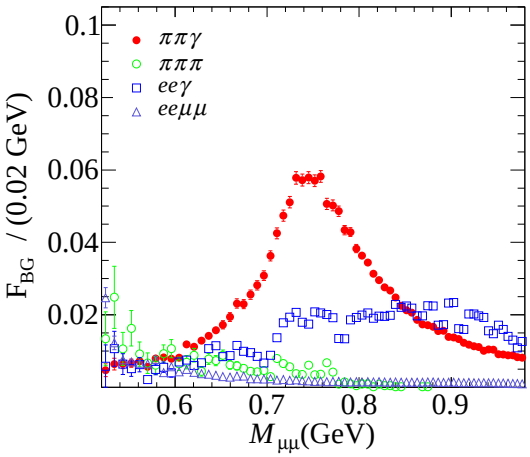

Fig. 1. Fractional backgrounds to the $\mu\mu\gamma$ signal from the $\pi^+\pi^-\gamma$, $\pi^+\pi^-\pi^0$, $e^+e^-\gamma$, and $e^+e^-\mu^+\mu^-$ channels, see insert for symbols.

$F_{\rm BG}$, contributing non negligibly (only statistical errors are shown), as a function of $M_{\mu\mu}$.

The accuracy of the $M_{\rm trk}$ determination depends on the quality of the fitted tracks. Since the left tail of the $M_{\rm trk}$ distribution for $e^+e^-\to\pi^+\pi^-\gamma$ contami-

nates the signal region, a cut on the error on $M_{\rm trk}$, $\sigma_{M_{\rm trk}}$, as obtained by the helix fit to the DC measured track points, improves the π/μ separation. The $\sigma_{M_{\rm trk}}$ distribution is correlated with $M_{\mu\mu}$, therefore we apply a $M_{\mu\mu}$-dependent $M_{\rm trk}$-cut (whose efficiency varies between 70 and 80% as function of $M_{\mu\mu}$). Figure 2 shows the cut in the $M_{\mu\mu}$, $\sigma_{M_{\rm trk}}$ plane. The $\sigma_{M_{\rm trk}}$ distribution for one slice

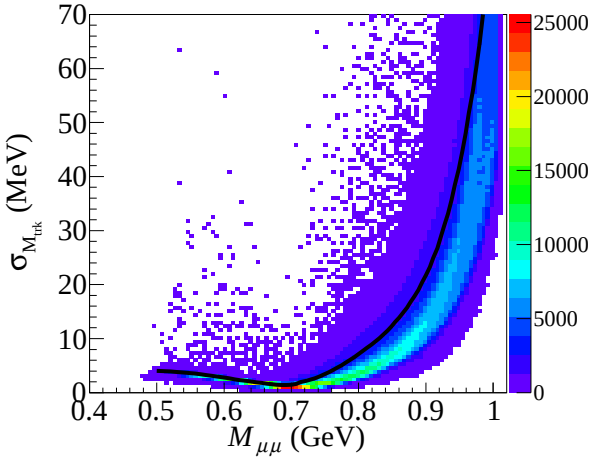

Fig. 2. Data scatter plot in the $M_{\mu\mu}$, $\sigma_{M_{\rm trk}}$ plane. Events above the solid line are rejected.

of $M_{\mu\mu}$ is shown in Fig. 3, left. Figure 3, right, shows the effect of this cut on the $M_{\rm trk}$ distribution, in the same $M_{\mu\mu}$ slice. There is a clear reduction of the left tail of the $\pi\pi\gamma$ $M_{\rm trk}$ signal, resulting in a reduction of the $\pi\pi\gamma$ background in the $\mu\mu\gamma$ $M_{\rm trk}$ region, slightly dependent on the $M_{\mu\mu}$ interval. Figure 3 also shows a good agreement between data and Monte Carlo simulation in both $\sigma_{M_{\rm trk}}$ and $M_{\rm trk}$ variables. After the cuts described the $M_{\mu\mu}$ spectrum con-

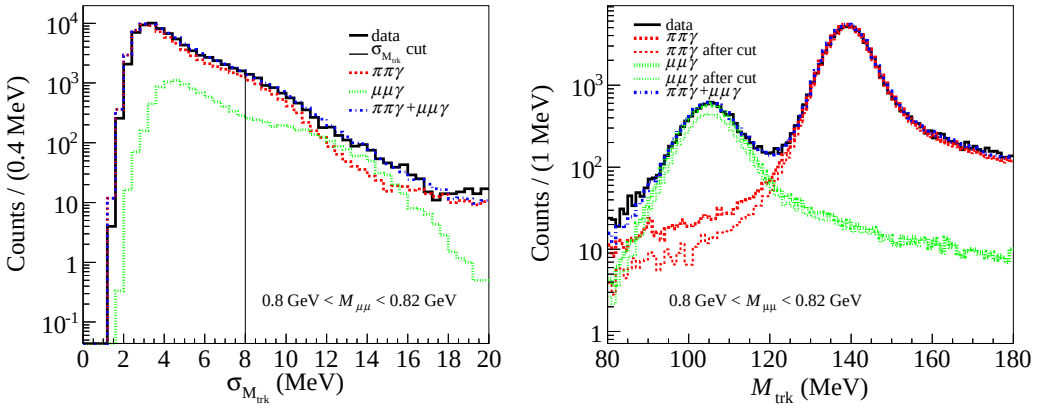

Fig. 3. Left: Distribution of $\sigma_{M_{\rm trk}}$ for one $M_{\mu\mu}$ slice for data, $\pi^+\pi^-\gamma$, $\mu^+\mu^-\gamma$ and the sum of $\pi^+\pi^-\gamma$ and $\mu^+\mu^-\gamma$. The $\sigma_{M_{\rm trk}}$ cut is also shown. Right: Effect of the $\sigma_{M_{\rm trk}}$ cut on $M_{\rm trk}$ distributions for the same slice of $M_{\mu\mu}$ for the $\pi^+\pi^-\gamma$ and $\mu^+\mu^-\gamma$, $M_{\rm trk}$ distributions without $\sigma_{M_{\rm trk}}$ cut. The corresponding thin lines show the effect of the $\sigma_{M_{\rm trk}}$ cut. All symbols are defined in the figures inserts.

sists of about 5.35×10^5 events. By correcting it for measurement/simulation

differences, subtracting the backgrounds and dividing by the efficiency and integrated luminosity [23], we obtain the differential cross section $\mathrm{d}\sigma_{\mu\mu\gamma}/\mathrm{d}M_{\mu\mu}$. Figure 4 left, shows the measured $\mu\mu\gamma$ cross section compared with the NLO QED calculations, using the MC code PHOKHARA [23]. Figure 4 right shows the ratio between the two differential cross sections fitted by a zero-degree polynomial. The agreement between measurement and the PHOKHARA simulation of the cross section is excellent.

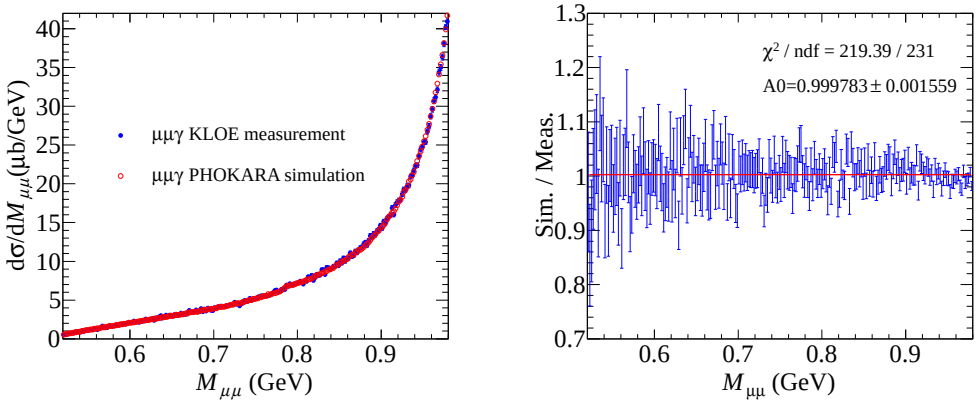

Fig. 4. Left: Comparison of data (full circles) and simulation (open circles) for $\mu^+\mu^-\gamma$ cross section; Right: Ratio of the two spectra with the results of a zero-degree polynomial fit.

3.1 Systematic errors and efficiencies

Several sources of systematic uncertainty contributing to the $\mu^+\mu^-\gamma$ event yield estimate have been evaluated.

Background subtraction: the systematic uncertainty is due to the background fit normalization parameters and the uncertainty on the $e^+e^-\mu^+\mu^-$ residual background. The total fractional systematic uncertainty, obtained by adding in quadrature the two contributions, ranges from 0.1 to 0.5%, decreasing with $M_{\mu\mu}$.

M_{trk} cut: the M_{trk} selection region for $\mu^+\mu^-\gamma$ is $80 < M_{\mathrm{trk}} < 115$ MeV. We varied the region boundaries by 5 MeV, and computed the ratio of the measured cross sections in the new region and in the region of standard cuts. The systematic uncertainty (constant in $M_{\mu\mu}$) is 0.4%.

$\sigma_{M_{\mathrm{trk}}}$ cut: the systematic uncertainty has been evaluated as the maximum difference between the $\mu\mu\gamma$ normalization parameters of the background fitting procedure, obtained with standard cuts, and those obtained by shifting $\sigma_{M_{\mathrm{trk}}}$ by $\pm 5\%$. The systematic contribution reaches the percent level (up to a maximum of 1.2%) at low $M_{\mu\mu}$ and decreases below 1% for $M_{\mu\mu} > 0.76$ GeV.

Acceptance: we estimate the uncertainty resulting from the angular acceptance cut for muons and photon to range from 0.1 up to 0.6%, by varying the limits by 1°.

Tracking: the single muon tracking efficiency, as function of the particle momentum and polar angle is obtained by a high purity $\mu^+\mu^-\gamma$ sample using one muon to tag the presence of the other. The combined efficiency is about 99%, almost constant in $M_{\mu\mu}$. The systematic uncertainty on tracking efficiency is evaluated changing the purity of the control sample and ranges from 0.3% to 0.6% as a function of $M_{\mu\mu}$.

Trigger: the trigger efficiency has been obtained from a sample of $\mu^+\mu^-\gamma$ events where a single muon satisfies the trigger requirement. Trigger response for the other muon is parameterized as a function of its momentum and direction. The efficiency as a function of $M_{\mu\mu}$ is obtained using the MC event distribution and differs from one by less than 10^{-3} for $M_{\mu\mu} < 0.6$ GeV and less than 10^{-4} for $M_{\mu\mu} > 0.6$ GeV.

Radiator function: we take as systematic uncertainty on H the value of 0.5%, as quoted in Ref. [20–23].

Luminosity: we calculated the luminosity using large-angle Bhabha scattering events [23], and evaluated the related systematic uncertainty to be 0.3%.

The dependence of the reconstruction efficiency, $\epsilon_{\rm eff}$, on $M_{\mu\mu}$ is shown in Fig. 5 (left). In Fig. 5 (right), we show the dependence of the total systematic uncertainty on the $\mu^+\mu^-\gamma$ yield.

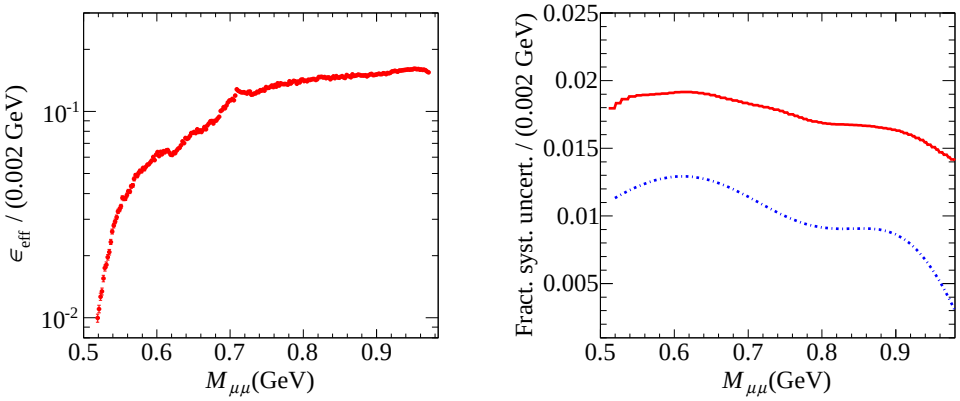

Fig. 5. Left: Global analysis efficiency, error bars are inside markers; Right: Total fractional systematic uncertainty on the expected $\mu\mu\gamma$ yield (solid line), the contribution due to the $\sigma_{M_{\rm trk}}$ cut only is shown by the dash-dotted line.

The largest contribution to total systematic error comes from the uncertainty on $\sigma_{M_{\rm trk}}$ cut, as shown by the dash dotted line in the figure.

4 Upper Limit on U-boson Coupling

U-boson decays into $\mu^+\mu^-$ would appear as a peak over the smooth $\mu^+\mu^-\gamma$ QED contribution. We find no evidence for a signal and we therefore set an upper limit on the kinetic mixing parameter ϵ^2 at 90% confidence level (CL).

We extract the limit on the number of U-boson candidates by using the CLS technique [31–33]. As *data* input for the limit extraction procedure, we use the observed invariant mass distribution. As *background* input, we used the $\mu^+\mu^-\gamma$ events simulated with PHOKHARA with the addition of the background sources reviewed in Section 3. The U-boson signal shape has been obtained from an appropriate generator. The signal width takes into account the resolution in $M_{\mu\mu}$ which varies from 1.5 MeV to 1.8 MeV, as $M_{\mu\mu}$ increases.

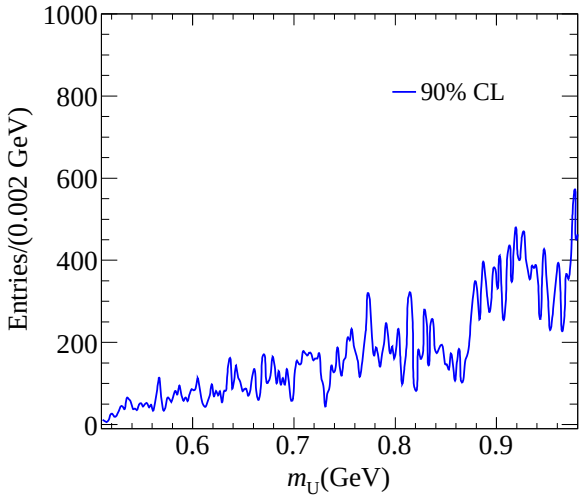

Fig. 6. Upper limit on the number of signal events at the 90% CL as function of the U-boson mass m_U.

Figure 6 shows the upper limit on the number of signal events at 90% CL, computed in steps of 2 MeV. A total systematic uncertainty between 1.4 and 1.8%, as shown in Fig. 5, has been applied to the background. Statistical uncertainties on data, expected background, and signal are also included in the procedure. We extract the limit on the kinetic mixing parameter by according to:

$$\epsilon^2 = \frac{(N_{\rm CLS} - B_{\rm exp})/(\epsilon_{\rm eff} \times L)}{H \times I}, \tag{2}$$

where $B_{\rm exp}$ is the background, $\epsilon_{\rm eff}$ represents the overall efficiency, L is the integrated luminosity, H is the radiator function and I is the effective cross section for $e^+e^- \to U \to \mu^+\mu^-$ integrated on a single mass bin with $\epsilon = 1$.

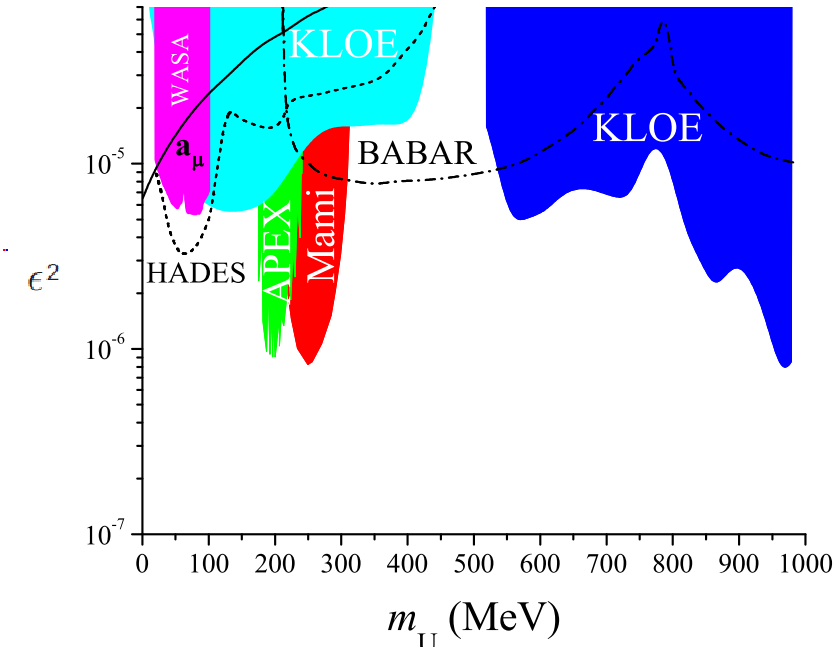

Fig. 7. 90% CL exclusion plot for ϵ^2 as a function of the U-boson mass (blue). The limits from the MAMI [34] (red) and Apex [35] (green) fixed-target experiments, the KLOE limit from $\phi \to e^+e^-\gamma$ [38] (cyan), the WASA [36] (magenta) and HADES [40] limits (dashed line) are also shown. The dash-dotted line is an estimate using BaBar data [18, 39]. The solid black line is a limit from the muon anomaly [41].

The resulting exclusion plot on the kinetic mixing parameter ϵ^2, in the 520–980 MeV mass range, is shown in Fig. 7. The sensitivity loss due to the ρ meson around 770 MeV is visible. In the same plot, other limits in the mass range below 1 GeV are also shown [18, 34–39]. The solid black line is a limit from the muon g-2 [41]. Our 90% CL limit is between 1.6×10^{-5} and 8.5×10^{-7} in the 520–980 MeV mass range.

5 Conclusions

We have searched for a light, dark vector boson in the $e^+e^- \to \mu^+\mu^-\gamma$ channel in a sample of 5.35×10^5 events recorded with the KLOE detector for a total integrated luminosity of 239.3 pb^{-1}. We find no evidence for a U Boson, in the mass range 520–980 MeV. The upper limit at 90% CL on the mixing parameter ϵ^2 is between 1.6×10^{-5} and 8.5×10^{-7}, ruling out a wide range of U-boson scenarios. The limit is derived through a study of the $\mu^+\mu^-\gamma$ ISR process and significantly improves the current limit on ϵ in the above mass range.

6 Acknowledgments

We warmly thank our former KLOE colleagues for the access to the data collected during the KLOE data taking campaign. We thank the DAΦNE team for their efforts in maintaining low background running conditions and their collaboration during all data taking. We wish to thank our technical staff: G.F. Fortugno and F. Sborzacchi for their dedication in ensuring efficient operation of the KLOE computing facilities; M. Anelli for his continuous attention to the gas system and detector safety; A. Balla, M. Gatta, G. Corradi and G. Papalino for electronics maintenance; M. Santoni, G. Paoluzzi and R. Rosellini for general detector support; C. Piscitelli for his help during major maintenance periods. This work was supported in part by the EU Integrated Infrastructure Initiative Hadron Physics Project under contract number RII3-CT- 2004-506078; by the European Commission under the 7th Framework Programme through the 'Research Infrastructures' action of the 'Capacities' Programme, Call: FP7-INFRASTRUCTURES-2008-1, Grant Agreement No. 227431; by the Polish National Science Centre through the Grants No. 0469/B/H03/2009/37, 0309/B/H03/2011/40, DEC-2011/03/N/ST2/02641, 2011/01/D/ST2/00748, 2011/03/N/ST2/02652, 2013/08/M/ST2/00323 and by the Foundation for Polish Science through the MPD programme and the project HOMING PLUS BIS/2011-4/3.

References

[1] B. Holdom, Phys. Lett. B 166 (1985) 196.

[2] C. Boehm, P. Fayet, Nucl. Phys. B 683 (2004) 219.

[3] Y. Mambrini, J. Cosmol. Astropart. Phys. 1009 (2010) 022.

[4] M. Pospelov, A. Ritz, M.B. Voloshin, Phys. Lett. B 662 (2008) 53.

[5] M. Pospelov, A. Ritz, Phys. Lett. B 671 391 (2009) 1502.

[6] N. Arkani-Hamed, et al., Phys. Rev.D 79 (2009) 015014.

[7] I. Cholis, et al., Phys. Rev. D 80 (2009) 123518.

[8] O. Adriani, et al., Nature 458 (2009) 607.

[9] M. Aguilar, et al. Phys. Rev. Lett. 110 (2013) 141102.

[10] P. Jean, et al., Astronomy Astrophysics 407 (2003) L55.

[11] J. Chang, et al., Nature 456 (2008) 362.

[12] F. Aharonian, et al., Phys. Rev. Lett. 101 (2008) 261104.

[13] A. A. Abdo, et al., Phys. Rev. Lett. 102 (2009) 181101.

[14] R. Barnabei, et al., Eur. Phys. J. C 56 (2008) 333.

[15] P. Fayet, Phys. Rev. D 75 (2007) 115017.

[16] R. Essig, P. Schuster, N. Toro, Phys. Rev. D80, (2009) 015003.

[17] B. Batell, et al., Phys. Rev. D79, (2009) 115008.

[18] M. Reece and L.T. Wang, JHEP 07, (2009) 051.

[19] L. Barzè, et al., Eur. Phys. J. C 71 (2011) 1680.

[20] G. Rodrigo, H. Czyż , J.H. Kühn, M. Szopa, Eur. Phys. J. C 24 (2002) 71.

[21] H. Czyż , A. Grzelinska, J.H. Kühn, G. Rodrigo, Eur. Phys. J. C 27 (2003) 563.

[22] H. Czyż , A. Grzelinska, J.H. Kühn, G. Rodrigo, Eur. Phys. J. C 33 (2004) 333.

[23] H. Czyż , A. Grzelinska, J.H. Kühn, G. Rodrigo, Eur. Phys. J. C 39 (2005) 411.

[24] S. Actis, et al., Working Group on Radiative Corrections and Monte Carlo Generators for Low Energies Collaboration, Eur. Phys. J. C 66 (2010) 585.

[25] M. Adinolfi, et al., Nucl. Instrum. Meth. A 488 (2002) 51.

[26] M. Adinolfi, et al., Nucl. Instrum. Meth. A 482 (2002) 364.

[27] M. Adinolfi, et al., Nucl. Instrum. Meth. A 492 (2002) 134.

[28] D. Babusci, et al., KLOE-KLOE2 Collaboration, Phys. Lett. B 720 (2013) 336.

[29] F. Ambrosino, et al., KLOE Collaboration, Phys. Lett. B 670 (2009) 285.

[30] F. Ambrosino, et al., KLOE Collaboration, Phys. Lett. B 700 (2011) 102.

[31] G. C. Feldman, R. D. Cousins, Phys. Rev. D 57 (1998) 3873.

[32] T. Junk, Nucl. Instr. Meth. A434 (1999) 435.

[33] A. L. Read, J. Phys. G: Nucl. Part. Phys. 28 (2002) 2693.

[34] M. Merkel, et al., Phys. Rev. Lett. 106 (2011) 251802.

[35] S. Abrahamyan, et al., Phys. Rev. Lett. 107 (2011) 191804.

[36] P. Adlarson, et al., WASA-at-COSY Collaboration, Phys. Lett. B 726 (2013) 187.

[37] F. Archilli, et al., Phys. Lett B706 (2012) 251.

[38] D. Babusci, et al., KLOE-KLOE2 Collaboration, Phys. Lett. B 720 (2013) 111.

[39] B. Aubert, et al., BaBar Collaboration, Phys. Rev. Lett. 103 (2009) 081803; J. D. Bjorken, R. Essig, P. Schuster, and N. Toro, Phys. Rev. D 80(2009) 075018.

[40] G. Agakishiev et al., HADES Collaboration, Phys. Lett. B 731 (2014) 265.

[41] M. Pospelov, Phys. Rev. D 80 (2009) 095002.